

# Organic & Biomolecular Chemistry

Accepted Manuscript



This is an *Accepted Manuscript*, which has been through the Royal Society of Chemistry peer review process and has been accepted for publication.

*Accepted Manuscripts* are published online shortly after acceptance, before technical editing, formatting and proof reading. Using this free service, authors can make their results available to the community, in citable form, before we publish the edited article. We will replace this *Accepted Manuscript* with the edited and formatted *Advance Article* as soon as it is available.

You can find more information about *Accepted Manuscripts* in the [Information for Authors](#).

Please note that technical editing may introduce minor changes to the text and/or graphics, which may alter content. The journal's standard [Terms & Conditions](#) and the [Ethical guidelines](#) still apply. In no event shall the Royal Society of Chemistry be held responsible for any errors or omissions in this *Accepted Manuscript* or any consequences arising from the use of any information it contains.

## INHIBITION OF HUMAN MITOCHONDRIAL AND CYTOSOLIC 5'(3')-DEOXYNUCLEOTIDASES BY CONFORMATIONALLY CONSTRAINED NUCLEOSIDE PHOSPHONIC ACIDS

Ondřej Šimák,<sup>1,&</sup> Petr Páchl,<sup>1,2,&</sup> Milan Fábry,<sup>2</sup> Miloš Buděšínský,<sup>1</sup> Tomáš Jandušík,<sup>1,3</sup> Aleš Hnízda,<sup>1</sup> Radka Skleničková,<sup>1</sup> Magdalena Petrová,<sup>1</sup> Václav Veverka,<sup>1</sup> Pavlína Řezáčová,<sup>1,2</sup> Jiří Brynda,<sup>1,2,\*</sup> Ivan Rosenberg<sup>1,\*</sup>

<sup>1</sup>*Institute of Organic Chemistry and Biochemistry, Academy of Sciences of the Czech Republic, v. v. i., Flemingovo 2, 166 10 Prague 6, Czech Republic; E-mail:*

*ivan@uochb.cas.cz*

<sup>2</sup>*Institute of Molecular Genetics, of Sciences of the Czech Republic, v. v. i., Videňská 1083, 14220 Prague 4, Czech Republic;*

<sup>3</sup>*Department of Chemistry of Natural Compounds, Institute of Chemical Technology, Prague, Technická 5, 166 28 Prague, Czech Republic*

**Keywords:** 5'(3')-nucleotidase, nucleoside phosphonates, inhibitor, crystal structure, substituted orthobenzoates.

**Abbreviations:** ALL, acute lymphoblastic leukemia; AML, acute myeloid leukemia; AZT, zidovudine; cdN, cytosolic 5'(3')-deoxynucleotidases; cN-II, cN-IA and cN-III, cytosolic 5'-nucleotidases; eN, ecto-5'-nucleotidase; FUDR, fludarabine, FdU, 5-fluoro-2'-deoxyuridine; FdUMP, 5-fluoro-2'-deoxyuridine 5'-phosphate;  $K_i$ , inhibition constant;  $K_M$ , Michaelis-Menten constant; mdN, mitochondrial 5'(3')-deoxynucleotidases; RMSD, root-mean-square deviation; SI, selectivity index

\* Corresponding authors: [rosenberg@uochb.cas.cz](mailto:rosenberg@uochb.cas.cz); [brynda@img.cas.cz](mailto:brynda@img.cas.cz); <sup>&</sup> both authors contributed to this work equally

**ABSTRACT:**

This work describes novel *in vitro* inhibitors of human mitochondrial (mdN) and cytosolic (cdN) 5'(3')-deoxynucleotidases. We designed a series of derivatives of the lead compound (*S*)-1-[2-deoxy-3,5-*O*-(phosphonobenzylidene)- $\beta$ -D-threo-pentofuranosyl]thymine bearing various substituents in the *para* position of the benzylidene moiety. Detailed kinetic study revealed that certain *para* substituents increase the inhibitory potency (iodo derivative;  $K_i^{\text{mdN}}=2.71 \mu\text{M}$ ) and some induce a shift in selectivity toward cdN (carboxy derivative,  $K_i^{\text{cdN}}=11.60 \mu\text{M}$ ; iodoxy derivative,  $K_i^{\text{cdN}}=6.60 \mu\text{M}$ ). Crystal structures of mdN in complex with three of these compounds revealed that various *para* substituents lead to two alternative inhibitor binding modes within the enzyme active site. Two binding modes were also identified for cdN complexes by heteronuclear NMR spectroscopy.

## INTRODUCTION

5'-Nucleotidases are catabolic enzymes that catalyze the dephosphorylation of nucleoside 5'-monophosphates. Together with nucleoside kinases and nucleoside phosphorylases, they regulate cellular nucleotide and nucleoside pools.<sup>1-3</sup> There are seven human 5'-nucleotidases with different substrate specificities, cellular localization, and tissue-specific expression patterns:<sup>1, 4, 5</sup> ecto-5'-nucleotidase (eN), cN-IA (AMP specific), cN-IB (AMP specific), cN-II (IMP and GMP specific), cN-III (CMP and UMP specific), and two 5'(3')-deoxynucleotidases—cytosolic (cdN) and mitochondrial (mdN). cdN is an ubiquitous enzyme that, in contrast to cN-III and mdN, is not strictly pyrimidine-specific and efficiently dephosphorylates dIMP and dGMP as well as dTMP and dUMP. In addition, cdN exhibits limited activity toward dAMP and no activity toward dCMP.<sup>6</sup> mdN is highly homologous to cdN (sequence homology of 78%) but has a remarkably narrow specificity toward dUMP and dTMP, which are considered to be its physiological substrates.<sup>7</sup> Its high pyrimidine specificity suggests that mdN regulates the level of mitochondrial dTTP and prevents the accumulation of mutagenic dUTP.<sup>6</sup>

In addition to their regulatory role, 5'-nucleotidases can dephosphorylate the 5'-phosphate esters of therapeutically relevant nucleoside analogs, thus negatively affecting their pharmacological efficacy. Both cdN and mdN are capable of efficiently dephosphorylating modified therapeutic nucleoside 5'-phosphates. In particular, cdN efficiently dephosphorylates the 5'-phosphates of zidovudine (AZT) and fludarabine (FUDR), which are used for HIV-1 and cancer (leukemias and solid tumors) treatment, respectively. The rate of cleavage of FdUMP, an active metabolite of fludarabine, is two-fold higher than the dUMP cleavage rate.<sup>6</sup>

Primary and acquired resistance toward nucleoside analogs is a limiting factor in their clinical use, and resistance seems to be linked to high expression and increased activity of cytosolic 5'-nucleotidases.<sup>7-9</sup> In particular, araC-resistant leukemia cell lines with increased

cN-II activity are less sensitive to fludarabine,<sup>10</sup> and recent results identified a relapse-specific activating mutation in cN-II in childhood acute lymphoblastic leukemia (ALL).<sup>11, 12</sup> In parallel, increased activity of cdN and cN-III was found in the cells of patients with acute myeloid leukemia (AML) and ALL, and patients with clinical remission of ALL had even higher cdN activity than at the time of diagnosis.<sup>13</sup>

Long-term treatment with antiviral and anticancer nucleoside drugs is accompanied in almost all cases by serious drug-induced health problems.<sup>14, 15</sup> This is a consequence of mitochondrial toxicity induced in certain tissues.<sup>16, 17</sup> Nucleoside analogs can serve as substrates for the less-selective mitochondrial DNA polymerase gamma, causing chain termination and mtDNA depletion.<sup>16, 17</sup> Avoiding mitochondrial toxicity would require nucleoside analogs (i) whose 5'-triphosphates possess a low affinity toward mitochondrial DNA polymerase and/or (ii) whose 5'-monophosphates are good substrates for mdN.<sup>18</sup> Alternatively, nucleoside analogs that are good substrates for mdN could be combined with a selective cdN inhibitor.

Therefore, human cdN can be considered a promising therapeutic target, as its inhibition may increase the effectiveness of chemotherapy and antiviral treatment. Selective inhibition of mdN should be further investigated for its effects on various tumor cell lines.

Nucleoside phosphonic acids with a noncleavable P-C linkage have been studied as potential inhibitors of various nucleotidases. The first nucleoside phosphonate inhibitors (**1a** and **1b**), which block the activity of 5'-nucleotidase from *Crotalus adamanteus* venom, were reported in 1973 by Hampton et al. (Fig. 1).<sup>19</sup> In 1998, Garvey et al.<sup>20</sup> described the ddTMP analog **2** (Fig. 1) as a potent inhibitor of rabbit heart cN-I with an apparent  $K_i$  of 63 nM. Recently, Meurillon et al.<sup>21</sup> reported an inhibition study of cN-II with a variety of cytosine and uracil nucleoside phosphonic acids (based on scaffold **3**) with millimolar  $K_i$  values.

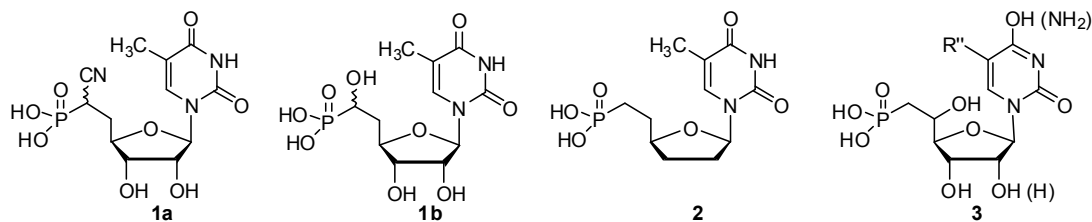


Figure 1. Chemical structures of nucleotide inhibitors of snake venom (**1a,b**), rabbit heart (**2**), and human cN-II 5'-nucleotidases (**3**).

Our group has synthesized many structurally diverse adenine, guanine, 2,6-diaminopurine, cytosine, uracil, and thymine nucleoside phosphonic acids.<sup>22-33</sup> Of these compounds, two types of structurally diverse nucleoside phosphonic acids, **4**<sup>34</sup> and **5**<sup>31, 32</sup> (Fig. 2), inhibited cdN and mdN.<sup>18, 35</sup> Whereas **4** inhibited both enzymes, **5** showed selectivity toward the mitochondrial enzyme.<sup>18</sup>

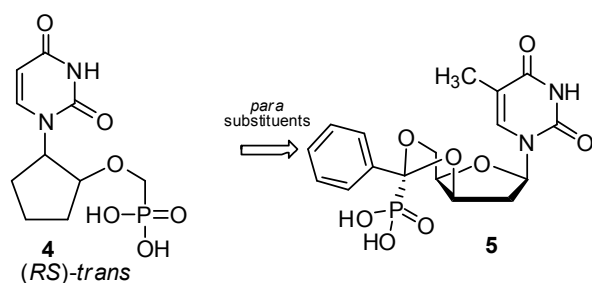


Figure 2. Two structurally diverse inhibitors of human cdN and mdN.

Detailed analysis of the crystal structures of mdN in complex with inhibitors **4** and **5**<sup>35</sup> showed that **4** binds to the enzyme active site in a manner similar to the natural 5'-nucleotide substrate, while the binding mode of **5** is different. The phosphonate moiety of **5** does not interact with the nucleoside phosphoester binding site but with another site distal from the catalytic residues.<sup>35</sup> A positively charged region formed by Arg163 and Arg177 and partially by Lys165 and Ser131 was identified in the vicinity of the *para* position of the benzylidene

ring in the crystal structure of the mdN-**5** complex.<sup>35</sup> With the aim of increasing inhibitor affinity, we designed a series of inhibitors with various substituents introduced at the *para* position of the benzylidene ring of **5**. At the same time, we focused on fine-tuning the inhibitor selectivity toward either cdN or mdN. Although the active sites of the two enzymes are very similar in terms of sequence and overall structure, detailed structural analysis revealed several regions with variable sequences<sup>36</sup> One variable region lies close to the positively charged region targeted by our proposed inhibitor substitutions. Specifically, this region comprises Ile133, Lys134, and Met135 in mdN (corresponding to cdN residues Leu202, Leu103, and Lys104). Also, Arg177 in mdN corresponds to Lys146 in cdN. This variability provides an opportunity for modification of the basal inhibitor scaffold to achieve specificity for cdN or mdN.

Here, we present novel inhibitors of human mdN and cdN based on (*S*)-1-[2-deoxy-3,5-*O*-(phosphonobenzylidene)- $\beta$ -D-threo-pentofuranosyl]thymine derivatives. We synthesized compounds with a series of polar electron-rich substituents (some with a negative charge) in the *para* position of benzylidene ring and tested these nucleoside benzylidenephosphonates for their inhibitory activity toward both enzymes. Structural characterization of inhibitor complexes with cdN and mdN revealed the existence of two alternative binding modes of the substituted compounds in the active site of both enzymes and emphasized the key role of the *para* substituent of the benzylidene moiety in determining the binding specificity. In addition, our data suggest that each of the isoenzymes requires a specific binding mode for effective inhibition.

## RESULTS AND DISCUSSION

**Chemistry.** The starting fifteen orthoesters **6a-o** (Table 1) were prepared in three steps from the corresponding *N,N*-methylphenylbenzamides.<sup>37</sup> The acid-catalyzed reaction of

orthoesters **6a-o** with *xylot* **7** in DMF yielded nucleoside orthobenzoates **9a-o** in high yield (Scheme 1). For the preparation of nucleoside orthoesters **9a-h**, we used dry HCl in Et<sub>2</sub>O as a catalyst, whereas for **9i-o**, pyridinium tosylate provided a much cleaner reaction without opening the nucleoside orthoester ring or forming a mixture of 3'- and 5'-*O*-acyl derivatives. In contrast to compounds **9a-h** and **9j**, which were obtained as single *R*-epimers, the compounds **9i** and **9k-o** were epimeric mixtures with the *R*-epimer prevailing (Fig. 3). NMR spectroscopy revealed that the furanose ring adopts an <sup>3</sup>*E* (*C3'*-*endo*) conformation, while the annealed 1,3-dioxane ring is in a chair conformation. Thus, the relatively bulky phenyl substituent is in an equatorial position on the six-membered 1,3-dioxane ring (Fig. 3). The use of a strong acid (HCl in Et<sub>2</sub>O) may lead to a quasi-reversible transesterification reaction: partial re-opening of the formed cyclic orthoester ring and repeated closure provides the thermodynamic products **9a-h**. On the other hand, the use of pyridinium tosylate as a weak acid maintains the intact cyclic orthoester ring affording the kinetic products. The epimeric mixtures of compounds **9i-o** (the obtained ratios from the NMR spectra are given in the Experimental section in Supplementary information).

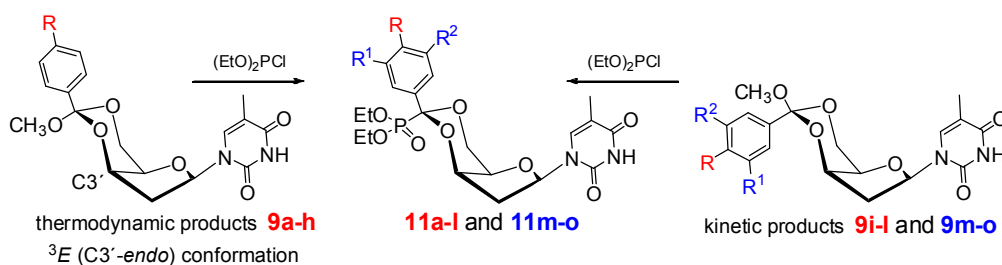
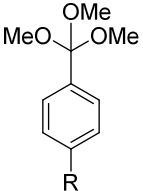
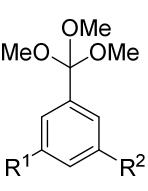
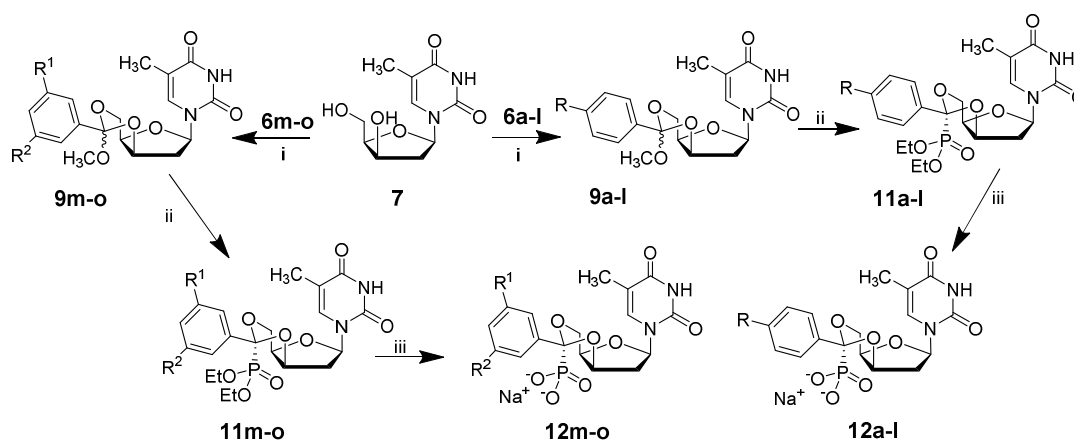


Figure 3. Configurations of the thermodynamic and kinetic products.

Table 1. Prepared orthobenzoates **6a-o**.



Compounds <b>6</b>	R	R	Compounds <b>6</b>	R <sup>1</sup> , R <sup>2</sup>
	<b>a</b> <sup>38</sup>	F	<b>g</b>	SMe
	<b>b</b> <sup>39</sup>	Cl	<b>h</b>	CN
	<b>c</b> <sup>39</sup>	Br	<b>i</b>	CF <sub>3</sub>
	<b>d</b>	I	<b>j</b> <sup>37</sup>	OCH <sub>3</sub>
	<b>e</b> <sup>37</sup>	NO <sub>2</sub>	<b>k</b>	vinyl
	<b>f</b>	COOMe	<b>l</b> <sup>41</sup>	Ph
	<b>m</b>	C <sub>6</sub> H <sub>5</sub> , H		
	<b>n</b> <sup>40</sup>	I, H		
	<b>o</b>	I, Br		



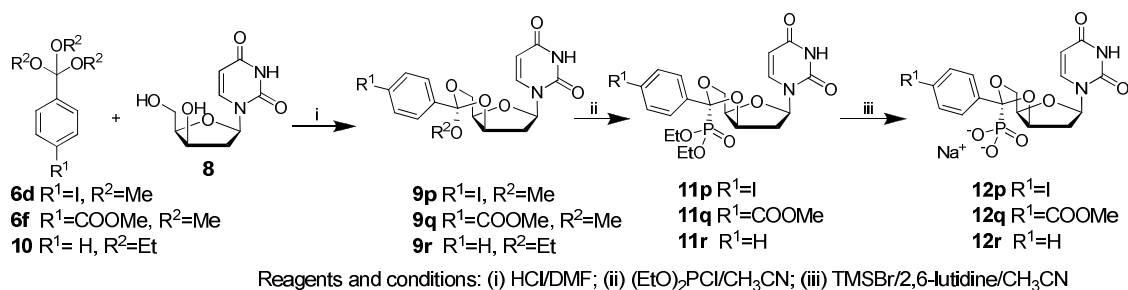
Reagents and conditions: (i) HCl/DMF or TsOH, py/DMF; (ii) (EtO)<sub>2</sub>PCl/CH<sub>3</sub>CN; (iii) TMSBr/2,6-lutidine/CH<sub>3</sub>CN; for R, R<sup>1</sup>, and R<sup>2</sup> see Table 1.

Scheme 1. Synthesis of substituted phosphonobenzylidene derivatives of 1-[2-deoxy-β-D-threo-pentofuranosyl]thymine.

The NMR spectra showed that compounds **9a-h** and **9j** were obtained as only single C6'-epimer, while compounds **9i** and **9k-o** were C6'-epimeric mixtures. The configuration at C6' was determined from the observed NOE contacts of the C(6')-OMe group and the <sup>1</sup>H chemical shifts of the C(5)-Me group of thymine and the H-3' of the furanose ring. The NOE contacts between C(6')-OMe and the H-6 of thymine could be observed only in the C6'-epimers with a [6'S] configuration, while for C6'-epimers with a [6'R] configuration, an NOE between C(6')-OMe and H-3' was observed (see Figure 3). In series **9a-o**, both epimers clearly differ in their <sup>1</sup>H chemical shifts of the C(5)-Me group of thymine and the H-3' of the

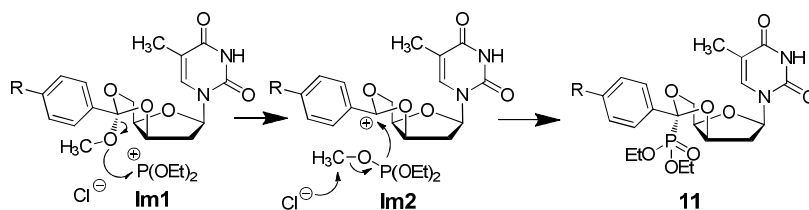
furanose ring. The C6'-epimers with a [6'R] configuration show a significant upfield shift of the signal belonging to the C(5)-Me group as a result of the shielding effect of the phenyl ring ( $\delta$  1.12 – 1.20 in [6'R] compared to  $\delta$  1.77 – 1.80 in the [6'S]-epimers). A reverse shielding effect is observed for H-3' ( $\delta$  4.27 – 4.35 in [6'S] compared to  $\delta$  4.66 – 4.71 in [6R]-epimers). The conformation of both C6'-epimers was studied by molecular modeling and theoretical calculations of the NMR parameters. Two potential chair conformations of the annealed 1,3-dioxane ring stabilize either the <sup>3</sup>E (C3'-endo) or the <sup>2</sup>E (C2'-endo) conformation of the furanose ring. Because the interproton coupling constants in **9a-o** are not influenced by the substitution of the aromatic ring at C6', we have chosen the C6'-epimers of **9i** as representative examples for a detailed conformational analysis of the of compounds **9a-o**. Geometric optimization was performed for both the C3'-endo and C2'-endo conformers of each C6'-epimer, and the optimized geometries were then used to calculate the <sup>1</sup>H and <sup>13</sup>C NMR chemical shifts using the same DFT B3LYP/6-31G\* method with an implicit solvent (PCM model; solvent = DMSO) in both steps. The vicinal couplings *J*(H,H) were calculated for the optimized geometries (shown in Fig. 5) with the MSpin program of the MESTRELAB package<sup>42</sup> using the Diez-Altona-Donders equation.<sup>43</sup> The comparison of the observed and calculated NMR parameters together with the calculated conformational data (*P* and  $\phi_{\max}$  of the furanose ring and the  $\chi$  angle for the nucleoside base orientation) and the relative energies of the C3'-endo and C2'-endo forms are given in Supplementary Table 1S. Mean average error values (MAE) are used to quantify the agreement between the observed and calculated data. As shown in Table 2, the relative energies, the comparison of the observed and calculated <sup>3</sup>*J*(H,H) values and the <sup>1</sup>H and <sup>13</sup>C chemical shifts clearly indicate that the C3'-endo conformation is highly preferred (>99%) for both the [6'R]- and [6'S]-epimers.

The reaction of xylodU **8** with orthoesters **6d**, **6f**, and **10** in DMF with 10 M HCl as an acid catalyst in Et<sub>2</sub>O yielded products **9p-r** exclusively as the *R*-isomers (Scheme 2).



Scheme 2. Synthesis of substituted phosphonobenzylidene derivatives of 1-[2-deoxy-β-D-threo-pentofuranosyl]uracil.

Similar stereoselective behavior was observed with the 3',5'-*O*-acetal derivatives of xyloT.<sup>27</sup> The reaction of nucleoside orthoesters **9a-r** with diethyl chlorophosphite in acetonitrile afforded the fully protected phosphonates **11a-r** as single epimers (**a-o** Scheme 1 and **p-r** Scheme 2). The stereospecificity of this reaction seems to be the result of the stable intermediate Im2 (Scheme 3) with the phenyl substituent in an equatorial position, which most likely subsequently undergoes an S<sub>N</sub>1 reaction to form diethyl methyl phosphite (Scheme 3). The proposed mechanism is similar to that of the previously reported mechanism for the formation of 2',3'-*O*-phosphonoalkylidene derivatives of ribonucleosides.<sup>32</sup>

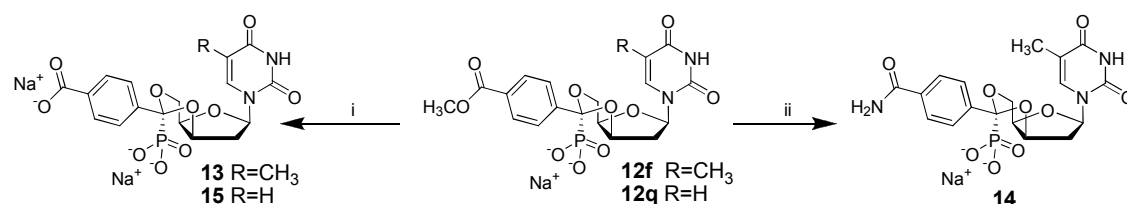


Scheme 3. Proposed mechanism of the stereospecific phosphorylation.

The deprotection of the phosphonate ester groups was carried out with bromotrimethylsilane in acetonitrile in the presence of 2,6-lutidine, providing phosphonic acids **12a-r** in moderate yields.

The carboxy derivative **13** was prepared in nearly quantitative yield by saponification of methyl ester **12f** in 0.5 M NaOH at r.t. The reaction of ester **12f** with 28% aqueous NH<sub>3</sub> at

100 °C for 24 h yielded carboxamide derivative **14** as the major product as well as free acid **13** (Scheme 4).

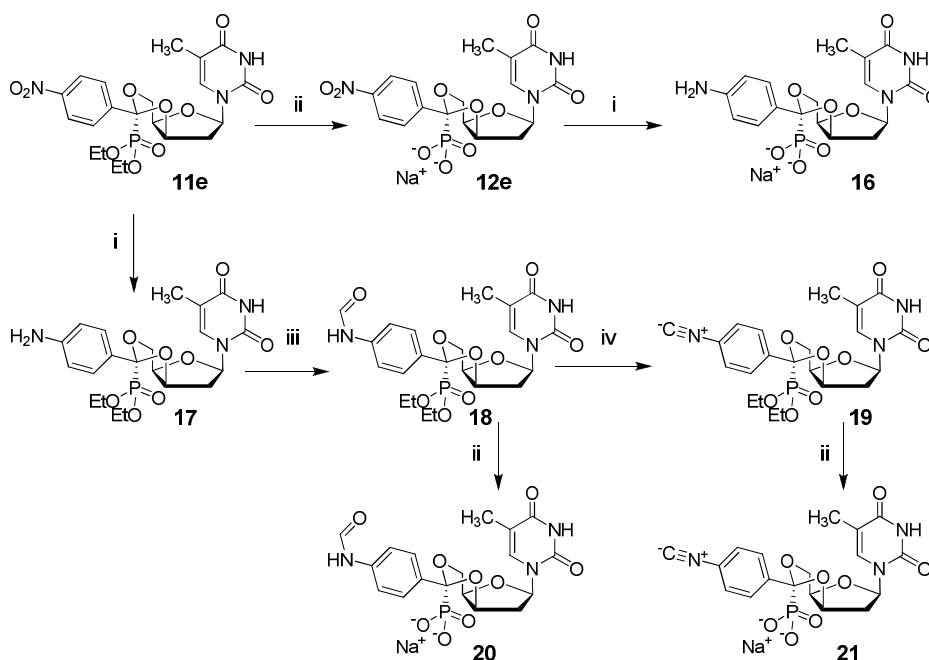


Reagents and conditions: (i) 0.05 M NaOH; (ii) 28% NH<sub>4</sub>OH/100°C/24 h.

Scheme 4. Transformation of the *para*-methoxycarbonyl group into carboxylate and carboxamide moieties.

The same reaction conditions were used for the preparation of carboxylate **15** from *para*-methoxycarbonyl derivative **12q** (Scheme 4).

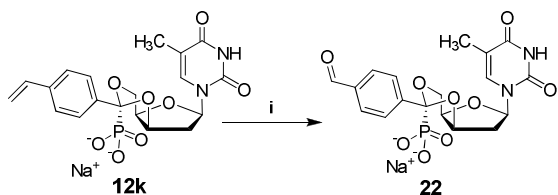
The catalytic hydrogenation of nitro derivatives **11e** and **12e** on Pd/C yielded the corresponding amino derivatives **16** and **17**, respectively. The obtained amino derivative **17** was converted to formamide **18** by reaction with ammonium formate in refluxing acetonitrile, and this compound yielded, in a subsequent reaction with phosphoryl chloride, isocyanide **19**. Amide **18** and isocyanide **19** were converted to free phosphonic acids **20** and **21**, respectively, by treatment with bromotrimethylsilane (Scheme 5).



Reagents and conditions: (i)  $\text{H}_2/\text{Pd-C}$ ; (ii)  $\text{TMSBr}/2,6\text{-lutidine}/\text{CH}_3\text{CN}$ ; (iii)  $\text{HCOONH}_4/\text{CH}_3\text{CN}$ ; (iv)  $\text{POCl}_3/\text{Et}_3\text{N}/\text{CH}_2\text{Cl}_2$

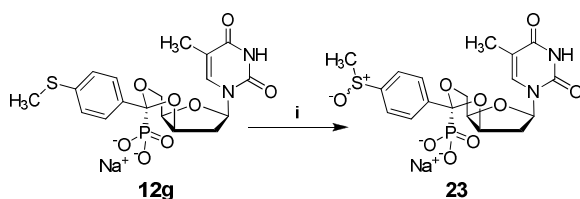
Scheme 5. Synthesis of the phosphonobenzylidene derivatives of 1-[2-deoxy- $\beta$ -D-threopentofuranosyl]thymine **16**, **20**, and **21**.

The synthesis of benzaldehyde derivative **22** (Scheme 6) started from styrene compound **12k**, which was oxidized by  $\text{OsO}_4$  in the presence of sodium periodate to afford **22** in nearly quantitative yield in one step. Similarly, a high yield of sulfoxide compound **23** was obtained by oxidation of the methylthio derivative **12g** with an aqueous solution of  $\text{NaIO}_4$  (Scheme 7).



Reagents and conditions: (i)  $\text{OsO}_4/\text{NaIO}_4/\text{tBuOH}/\text{H}_2\text{O}$

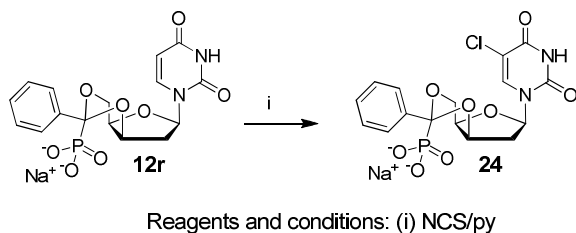
Scheme 6. Synthesis of 4-formylbenzylidene derivative **22**.



Reagents and conditions: (i)  $\text{NaIO}_4/\text{H}_2\text{O}$

Scheme 7. Synthesis of sulfoxide derivative **23**.

The chlorination of the uracil base<sup>44</sup> of derivative **12r** by *N*-chlorosuccinimide in pyridine at elevated temperature provided 5-chlorouracil derivative **24** (Scheme 8).



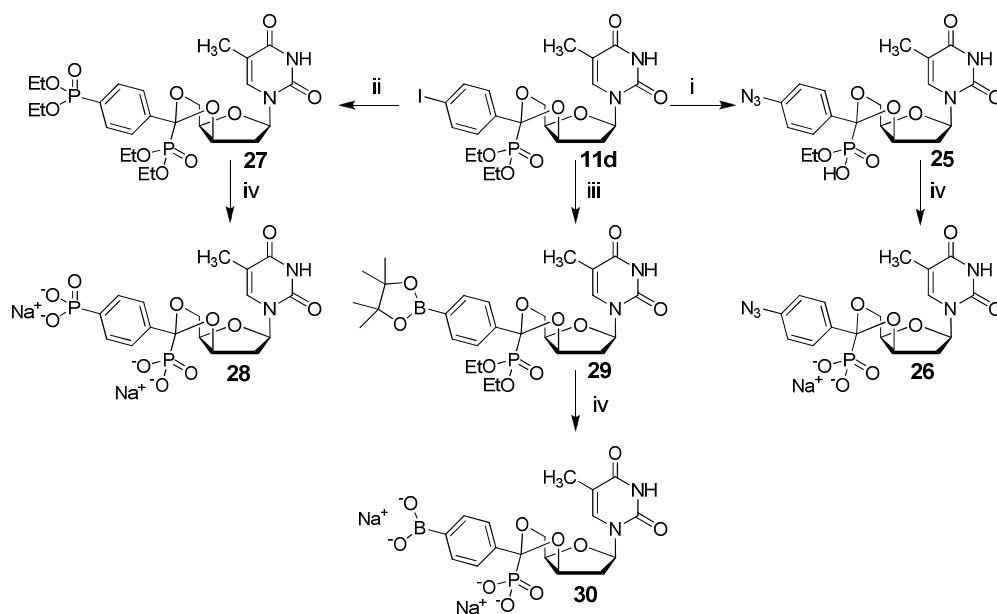
Scheme 8. Synthesis of 5-chlorouracil derivative **24**.

Iodophenyl derivative **11d** was a useful starting material for several transformations on the phenyl ring (Scheme 9).

Thus, compound **11d** was treated<sup>45</sup> with  $\text{NaN}_3$ , L-ascorbic acid, L-proline and  $\text{CuSO}_4$  in aqueous DMSO to yield azido derivative **25** as the mono ethyl phosphonate. This derivative was treated with TMSBr and 2,6-lutidine to provide phosphonic acid **26**.

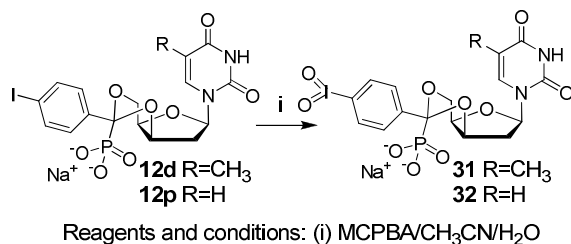
The coupling reaction<sup>46</sup> of **11d** with diethyl phosphite, catalyzed by  $\text{Pd}(\text{dppf})\text{Cl}_2$ , yielded tetraethyl diphosphonate **27**, which afforded bisphosphonic acid **28** on treatment with TMSBr and 2,6-lutidine.

The coupling reaction<sup>47</sup> of **11d** and bis(pinacolato)diboron, catalyzed by  $\text{Pd}_2(\text{dba})_3$  and XPhos, yielded boron derivative **29**. Its treatment with TMSBr and 2,6-lutidine afforded boronic acid **30**.



Scheme 9. Synthesis of azido compounds **25** and **26** and phosphoryl **28** and boronate **30** derivatives.

Iodophenyl derivatives **12d** and **12p**, as the free acids, were oxidized by *meta*-chloroperbenzoic acid, providing iodoxy derivatives **31** and **32**, respectively (Scheme 10).



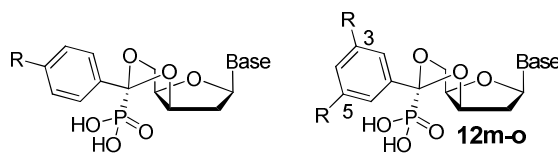
Scheme 10. Synthesis of iodoxy compounds **31** and **32**.

## Biochemistry

**Inhibition studies.** All synthesized phosphonic acids, as well as lead compound **5**, were screened for their inhibitory effect on mdN and cdN activity *in vitro* (Table 2). Activity assay was based on hydrolysis of dUMP in the presence of tested compounds. Substrate concentrations for preliminary tests were chosen to be similar to  $K_M$  (1 mM for cdN, 100  $\mu\text{M}$

for mdN) and concentration of tested compounds was 10 times lower than substrate concentration. Seventeen selected compounds that showed similar or lower relative enzyme activity  $v_i/v_0$  than lead compound **5** were subjected to a kinetic study to obtain the  $K_i$  values (Table 2). To compare the selectivity of the inhibitors toward mdN and cdN, we introduced a selectivity index (SI), defined as the ratio of  $K_i$  values normalized by the appropriate enzymatic constant  $K_M$ , which was determined experimentally ( $86 \pm 14 \mu\text{M}$  for mdN and  $968 \pm 79 \mu\text{M}$  for cdN). The smaller the SI ( $<1$ ) is, the higher selectivity of the inhibitor for mdN is, and the higher the SI ( $>1$ ) is, the higher the selectivity for cdN is.

Table 2. Inhibition of mitochondrial and cytosolic nucleotidases by benzylidene ring *para*-substituted derivatives of (*S*)-1-[2-deoxy-3,5-*O*-(phosphonobenzylidene)- $\beta$ -D-threopentofuranosyl] derivatives of pyrimidine nucleobasis.



R	Base	Cmpnd	Relative activity $v_i/v_0^a$		$K_i$ ( $\mu\text{M}$ )		$K_i/K_M$		Selectivity index <sup>b</sup>
			mdN	cdN	mdN	cdN	mdN	cdN	
	T	<b>5</b>	0.61	0.67	11.6 $\pm$ 2.0	610 $\pm$ 125	0.156	0.630	0.25
H	U	<b>12r</b>	0.44	0.97	31.1 $\pm$ 3.1	410 $\pm$ 120	0.362	0.424	0.85
	U <sup>5-Cl</sup>	<b>24</b>	0.69	0.56	11.8 $\pm$ 0.87	52.2 $\pm$ 4.5	0.137	0.054	2.5
F	T	<b>12a</b>	0.55	1.19	13.0 $\pm$ 1.9	n.d.	0.151	n.d.	n.d.
Cl	T	<b>12b</b>	0.63	1.03	30 $\pm$ 15	n.d.	0.349	n.d.	n.d.
Br	T	<b>12c</b>	0.79	0.82	31.8 $\pm$ 9.8	n.d.	0.370	n.d.	n.d.
	T	<b>12d</b>	0.42	0.82	2.71 $\pm$ 0.42	416 $\pm$ 66	0.032	0.430	0.073
	U	<b>12p</b>	0.72	0.66	19.7 $\pm$ 4.1	115 $\pm$ 11	0.229	0.119	1.9
I	T	<sup>c</sup>	0.69	0.81	14.2 $\pm$ 2.9	307 $\pm$ 38	0.165	0.317	0.52
	T	<b>11d</b>	0.81	0.77	n.d.	n.d.	n.d.	n.d.	n.d.
	T	<b>31</b>	0.44	0.07	5.90 $\pm$ 1.1	6.60 $\pm$ 1.4	0.069	0.0068	10
IO <sub>2</sub>	U	<b>32</b>	0.73	0.18	43.0 $\pm$ 11	12.1 $\pm$ 1.5	0.500	0.0125	40
NO <sub>2</sub>	T	<b>12e</b>	0.58	0.71	22.1 $\pm$ 3.3	950 $\pm$ 370	0.257	0.981	0.26



COOH	T	<b>13</b>	0.73	0.44	7.90	$\pm 2.2$	11.6	$\pm 1.7$	0.092	0.0120	7.7
	U	<b>15</b>	0.70	0.22	16.9	$\pm 2.1$	11.0	$\pm 0.86$	0.197	0.0114	17
COOMe	T	<b>12f</b>	0.96	1.01	n.d.		n.d.		n.d.	n.d.	n.d.
CONH <sub>2</sub>	T	<b>14</b>	0.77	0.92	n.d.		n.d.		n.d.	n.d.	n.d.
CHO	T	<b>22</b>	0.80	0.73	n.d.		n.d.		n.d.	n.d.	n.d.
CN	T	<b>12h</b>	0.54	0.77	23.0	$\pm 2.6$	177	$\pm 28$	0.267	0.183	1.5
P(O)(OH) <sub>2</sub>	T	<b>28</b>	0.69	0.54	28.0	$\pm 2.0$	52.7	$\pm 4.7$	0.326	0.054	6.0
B(OH) <sub>2</sub>	T	<b>30</b>	0.74	0.70	n.d.		n.d.		n.d.	n.d.	n.d.
SCH <sub>3</sub>	T	<b>12g</b>	0.57	0.98	33.3	$\pm 4.3$	n.d.		0.387	n.d.	n.d.
S(O)CH <sub>3</sub>	T	<b>23</b>	0.81	0.88	n.d.		n.d.		n.d.	n.d.	n.d.
NH <sub>2</sub>	T	<b>16</b>	0.89	0.82	n.d.		n.d.		n.d.	n.d.	n.d.
NHCHO	T	<b>20</b>	0.69	0.72	n.d.		n.d.		n.d.	n.d.	n.d.
NC	T	<b>21</b>	1.12	1.07	n.d.		n.d.		n.d.	n.d.	n.d.
N <sub>3</sub>	T	<b>26</b>	0.79	0.79	n.d.		n.d.		n.d.	n.d.	n.d.
CF <sub>3</sub>	T	<b>12i</b>	1.05	0.94	n.d.		n.d.		n.d.	n.d.	n.d.
OCH <sub>3</sub>	T	<b>12j</b>	1.20	0.80	n.d.		n.d.		n.d.	n.d.	n.d.
phenyl	T	<b>12l</b>	1.11	0.78	n.d.		n.d.		n.d.	n.d.	n.d.
3-phenyl	T	<b>12m</b>	0.72	0.82	n.d.		n.d.		n.d.	n.d.	n.d.
3-I	T	<b>12n</b>	0.87	0.64	n.d.		n.d.		n.d.	n.d.	n.d.
3-Br-5-I	T	<b>12o</b>	1.19	0.85	n.d.		n.d.		n.d.	n.d.	n.d.

<sup>a</sup> Values were obtained for a ratio of the substrate (dUMP) to inhibitor 10:1 at substrate concentrations of 100  $\mu\text{M}$  (mdN) and 1 mM (cdN); <sup>b</sup> the selectivity index  $[(K_i/K_M)_{\text{mdN}}/(K_i/K_M)_{\text{cdN}}]$  is expressed as a ratio of the  $K_i$  values for the mdN and cdN enzymes normalized to the enzymatic constant  $K_M$  of the individual enzymes  $[(K_M)_{\text{mdN}} = 86 \pm 14 \mu\text{M}, (K_M)_{\text{cdN}} = 968 \pm 79 \mu\text{M}]$ ; <sup>c</sup> mono-ethyl ester of **12d**.

The inhibitory effect of compound **5** on mdN had been previously investigated by others, and a  $K_i$  value of 70  $\mu\text{M}$  had been determined using specific assays with labeled dUMP.<sup>18</sup> In our HPLC assay, we followed the quantity of 2'-deoxyuridine released from dUMP by a nucleotidase-catalyzed hydrolysis. This method provided a  $K_i$  value for compound **5** and mdN of  $11.6 \pm 1.6 \mu\text{M}$ . A mixed inhibition mode for compound **5** was proposed from the analysis of the linearized Lineweaver-Burk plots. For the analysis of the inhibition mode, we did not use the Lineweaver-Burk plots because of the possible misinterpretation of the linearized data described for tightly binding inhibitors.<sup>48</sup> Instead, we used a non-linear regression fit of the

non-transformed data into the Williams-Morrison equation for the respective inhibition modes. The direct comparison of the inhibition data fit into the equations describing competitive, uncompetitive and noncompetitive<sup>48</sup> inhibition modes clearly indicated the competitive inhibition of mdN and cdN by compound **5**.

The introduction of iodo, iodoxy and carboxy substituents onto the *para* position of the phenyl ring of lead compound **5** improved the inhibitory effect of the iodo compound **12d**, iodoxy compound **31**, and carboxy compound **13** toward mdN by factors of five, two and 1.7, respectively (Table 2). In contrast to carboxy derivative **13**, aldehyde **22**, which could form a hemiacetal linkage with the hydroxyl of Ser131, showed weak inhibition activity. The inhibitory effect of iodo compound **12d** toward the cdN enzyme was not significantly affected; therefore, its selectivity toward mdN is more than three times higher compared to that of lead compound **5**. On the other hand, the presence of many other substituents improved the inhibition of cdN. Specifically, the compounds bearing iodoxy (**31**, **32**) and carboxy (**13**, **15**) groups showed the highest inhibition of cdN, with  $K_i$  values more than a hundred times lower than that of lead compound **5**. Additionally, the selectivity towards cdN changed dramatically; in the case of iodoxy derivative **32**, the selectivity index reached a value of 40 (Table 2, Supplementary Figure 3S).

The additional preference of mdN to bind the thymine over the uracil inhibitors was identified by comparing the  $K_i$  values of the compounds with the same substituent on the phenyl moiety but a different nucleobase (compounds **5/12r**, **12d/12p**, **13/15**, and **31/32**). However, an analogous preference for cdN was not established due to the lack of structural information.

We also evaluated the inhibition properties of two anionic compounds related to carboxy compound **13**: dihydroxyboryl derivative **30** and phosphoryl derivative **28** bearing an additional phosphoryl group. Compound **30**, which could form a hemiacetal bond with the

Ser131 hydroxy group and thus strengthen binding of **30** to the catalytic site, exhibited only weak inhibition. On the other hand, the phosphoryl derivative **28** was less than half an order of magnitude weaker than carboxy derivative **13** for inhibition of both enzymes but showed selectivity for cdN (SI = 6).

**Structural studies.** To determine the binding mode and interactions contributing to the inhibitory properties of this class of compounds, selected compounds were soaked into a crystal of mdN. The crystal structures of the mdN complexes with **12d**, **12e**, and **13** were determined by a difference Fourier technique using the structure of free mdN as a model (PDB code 4L6A<sup>36</sup>). The statistics for the diffraction data and structure refinements are summarized in Supplementary Table 3S. In all cases, the asymmetric unit contained one molecule of mdN with one compound bound in the active site. All mdN residues could be traced in a well-defined electron density map.

The structure of the complex with iodo compound **12d**, the most potent inhibitor of mdN from our series, was refined using diffraction data to a resolution of 1.78 Å. The electron density map used to model the inhibitor was of excellent quality (Figure 4A); the occupancy factor for the inhibitor was reduced to 0.85 to correctly explain the density.

The structure of the mdN complex with **12e** was refined using diffraction data to a resolution of 1.37 Å. The electron density map used for inhibitor placing clearly showed the position of the inhibitor, which was modeled with an occupancy factor of 0.7 (Figure 4C). Other non-protein electron densities in the active sites of the structures were modeled as phosphate and magnesium ions (Figure 4). The phosphate ion originated from the crystallization solution, which contained 20 mM potassium phosphate. Phosphate binding was

observed in the other structure of the free enzyme (PDB codes 1MH9,<sup>49</sup> 4L6A<sup>36</sup>) and in the structure of the mdN complex with compound **5** (PDB code 1Q92<sup>35</sup>).

The structure of the mdN complex with carboxy derivative **13** was refined to a resolution of 1.67 Å using diffraction data. The electron density map of the active site of the protein shows two alternative arrangements of ligands in the enzyme active site: carboxy compound **13** with an occupancy factor of 0.6 is overlaid with a phosphate ion with an occupancy factor of 0.4. Interestingly, the magnesium ion in this structure was replaced by a potassium ion (Figure 4E). The identity of the metal ion was confirmed by the level of the electron density map and also by the coordinating distances (Supplementary Table 3S).

The binding modes of iodo compound **12d** and nitro compound **12e** are similar to each other (Figure 4 A, C); the phosphonate group interacts with the areas of the active site distal from the catalytic residues, while the base moiety is deeply buried in the active site. This binding mode is very similar to that of compound **5**, as published by others;<sup>35</sup> the root-mean-square deviations (RMSD) for the superposition of the 28 corresponding atoms of **5** with **12d** and **12e** are 0.407 and 0.614 Å, respectively.

Although similar in structure, carboxy compound **13** binds to the mdN active site differently from **12d** and **12e**, with the phosphonate group coordinating to the catalytic magnesium ion. This binding pose is unique among all published mdN inhibitors<sup>35</sup> and resembles the binding mode of substrates (2'-deoxythymidine, uridine, and 2'-deoxyuridine 5'-monophosphates) in crystal structures of D41N (PDB codes 1Z4L, 1Z4M, and 1Z4I, Figure 4F).<sup>50</sup>

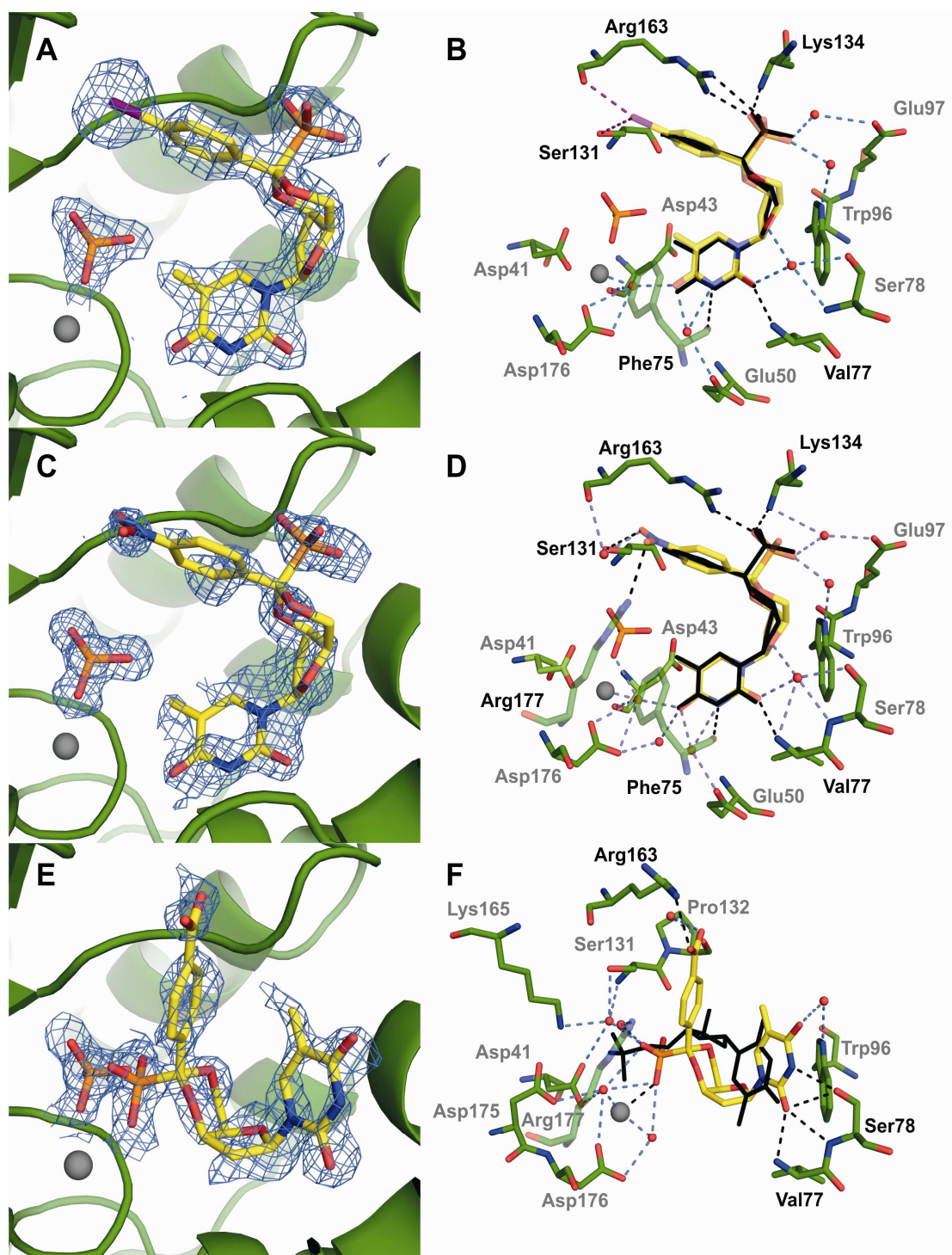


Figure 4. Details of the active site of the enzyme in crystal structures of mdN complexes with **12d** (panels A, B), **12e** (C, D), and **13** (E, F). The inhibitors are shown as stick models, and carbon atoms are yellow, oxygen atoms are red, nitrogen atoms are blue, phosphorus atoms are orange and iodine atoms are purple. In the protein, the carbon atoms are colored green. Phosphate and magnesium ions bound to the enzyme are also shown as sticks and balls,

respectively. In panels A, C and E, the  $2F_{\text{O}}-F_{\text{C}}$  electron density map is contoured at  $1.0\sigma$ . In panels B, D and F, the polar interactions between the inhibitor and mdN are represented by dashed lines. Direct hydrogen bonds and water-mediated hydrogen bonds are colored black and light blue, respectively. Halogen bonds in panel B are shown in purple. Residues participating in direct and water-mediated hydrogen bonds are named in black and gray, respectively. In panels B and D, the structure of lead compound **5** from crystal structure 1Q92<sup>35</sup> is shown in black lines. In panel F, the structure of the substrate analog from crystal structure 1Z4L<sup>50</sup> is shown in black.

Iodo compound **12d** and nitro compound **12e** participate in numerous polar interactions with the mdN active site (Figure 4B, D), and most of them are analogous to the interactions described previously for compound **5**.<sup>35</sup> The thymine base 3-*NH* group of **12d** or **12e** forms a hydrogen bond with the main chain carbonyl of Phe75. The O2 carbonyl oxygen of the thymine forms a hydrogen bond with the main chain amide of Val77 and a water-mediated hydrogen bond with the Ser78 hydroxyl group. The carbonyl oxygen at C4 of the base forms bonds with two water molecules; one of them is coordinated by a  $\text{Mg}^{2+}$  ion, and the other water forms a hydrogen bond with a carboxyl group of Glu50. The polar interactions of the pentofuranosyl moiety of **12d** or **12e** include one water-mediated hydrogen bond to Ser78 and the interaction of the hydrogen atoms at C1' and C2' with the  $\pi$ -electrons of the Trp96 aromatic side chain. The phosphonate groups of **12d** and **12e** bind to a positively charged pocket and form direct hydrogen bonds with the main chain amide of Lys134 and the side chains N $\eta$ 1 and N $\eta$ 2 of Arg163. Additionally, the phosphonate group forms water-mediated hydrogen bridges with Glu97 and Trp96.

The iodo or nitro substituents at the *para* position of the phenyl ring provide additional interactions not present in complexes with lead compound **5**. The iodo group of **12d** forms two halogen bonds<sup>51, 52</sup> (Figure 4B). The first interaction is with a partially negatively charged carbonyl oxygen of Arg163 at distance of 3.6 Å with a C-I-O angle of 166°. The second interaction, is the hydrogen bond with the hydroxyl group of the Ser131 side chain (distance

4.0 Å, C-I-O angle 106°). The bond distances and angles are in agreement with the values expected for the interaction of a halogen with a Lewis base (carbonyl oxygen) and a Lewis acid (H-atom of the hydroxyl group).<sup>51-53</sup>

The nitro group of **12e** forms direct hydrogen bonds with the side chains of Ser131 and the Nη1 atom of Arg177. The larger volume of the nitro group compared to the iodine in **12d** results in a slight shift of the nitrophenyl moiety away from Ser131 (0.47 Å) and also a small rotation (~15.4°) of the phosphonate group (Figure 4D). Because of this small structural change, the hydrogen bond network of the **12e** phosphonate group differs marginally from those in **12d** and **5**.

In compound **13**, the phosphonate group is buried in the mdN active site and contributes to the coordination of the potassium ion (Figure 4F). In addition, several water-mediated hydrogen bonds are formed between the phosphonate group and Asp41, Ser131, Lys165, Asp175, Asp176, and Arg177. The base moiety forms direct hydrogen bonds via the N3 atom with the Ser78 hydroxyl group and via the O2 atom with the main chain amide of Val77. A water-mediated hydrogen bond is also formed between the base carbonyl and Trp96. The carboxyl group at the *para* position of the phenyl ring forms one direct hydrogen bond with the guanidine group of Arg163 and one water-mediated hydrogen bond with the carbonyl of Pro132.

We have characterized the interactions of cdN with selected compounds (**12d**, **13**, **15**, **31** and **32**) using protein-detected NMR spectroscopy, as the extensive soaking trials did not yield crystals of cdN with bound small molecules. cdN provides well-resolved NMR spectra, which allowed for the backbone resonances to be completely assigned.<sup>54</sup> The effects of the added compounds were followed using 2D <sup>15</sup>N/<sup>1</sup>H TROSY spectra of <sup>15</sup>N-labeled cdN. The chemical shift perturbations induced by the selected compounds are summarized as graphs of the minimal shift values (Figure 2S; Supporting Information). As expected, the most

perturbed residues were localized around the active site of cdN, suggesting that all the tested compounds bind to the same region of the enzyme, possibly with similar conformations. In particular, two regions of cdN, Gly13-Asp16 and Phe44-Arg47, were found to be consistently affected by all inhibitors. However, a detailed analysis revealed certain differences in the distribution of changes in the cdN backbone signal positions upon binding of various compounds. Significant differences were first observed between compounds **12d** and **13**; **12d** affected Arg47, and **13** strongly perturbed the signal from Arg132 and its neighboring residues Thr131, Asp133, Lys134 and Thr135. Considering the relatively small difference between the covalent structures of **12d** and **13**, the distribution of the compound-specific local changes observed in the cdN spectra suggests a different orientation of these compounds in the active site, with the carboxylic group of **13** displacing the side chain of Arg132 in a manner similar to that observed in the X-ray structure of the complex with mdN (Figure 4F); **12d** adopts the reverse orientation. The presence of two different binding modes for the highly similar compounds **12d** and **13** is further supported by the difference of > 2 ppm between the positions of the  $^{31}\text{P}$  signals from the phosphonate groups in the 1D  $^{31}\text{P}$  NMR spectra obtained for both complexes. Compound **15** showed overlapping perturbations with **13** within the region around Arg132, although there were additional changes in other residues, including Val61-Phe71 and Lys104-His106, suggesting that different contacts were established by the uracil base (**15**) compared with the thymine base of **13**. The additional effects of **31** and **32** cannot be unambiguously interpreted.

## CONCLUSION

We have shown that the introduction of various substituents into the *para* position of the phenyl ring of the mdN-specific inhibitor **5** can lead to improvement in the inhibitory activity toward mdN and also fine tune the selectivity toward cdN. To our knowledge, compounds



**12d** and **31**, with different substituents (iodo and iodoxy), are the most potent and specific inhibitors of mdN and cdN, respectively, reported to date. On the other hand, uracil iodoxy compound **32** exhibited four times higher selectivity index towards cdN than compound **31**, suggesting the important role of the pyrimidine nucleobase type on the selectivity (compare also **12d** and **12p**).

The crystallographic data provided evidence for the existence of two different binding orientations for compounds **12d** and **13** in the active site of mdN and underlined the crucial role of the substituent on the binding specificity. The NMR data obtained for the analogous cdN complexes confirmed similar binding behavior. Based on the inhibition kinetics and structural data, we propose that inhibitors more specific towards mdN are preferentially binding to the mitochondrial and cytosolic enzyme in the orientation represented by lead compound **5**, while for inhibitors more specific towards cdN, the proteins favor the opposite orientation, similar to that observed for the complex of mdN with compound **13**. This suggests that each of the isoenzymes requires a specific binding mode for effective inhibition.

### Acknowledgements

Financial support by Grant 203/09/0820, 13-24880S, 13-26526S (Czech Science Foundation) and by Research Centers KAN200520801 (Acad. Sci. CR) is gratefully acknowledged. This work was also supported in part by projects RVO 61388963 and 68378050 awarded by the Academy of Sciences of the Czech Republic and by the Ministry of Education of the Czech Republic - LK11205 (programme “NAVRAT”). The authors are indebted to Eva Zborníková, MSc. for LC-MS measurements and the staff of the Mass Spectrometry Department of Institute of Organic Chemistry and Biochemistry AS CR (Dr.

Josef Cvačka, Head) and Zdeněk Fiedler for the measurements and interpretations of HR mass spectra and IR spectra.

**Supporting information available:** (1) Calculated geometry and NMR parameters for *C3'*-*endo* and *C2'*-*endo* conformations of [6'*R*] and [6'*S*]-epimers of compound **9i**. (2) Backbone NMR chemical shift perturbations obtained for cdN complexes (compounds **12d**, **13**, **15**, **31** and **32**). (3) Calculated distances of metal ion and coordinating atoms in 3 different structures. (4) Selectivity graph of measured compounds. (5) Experimental section

### References:

1. S. A. Hunsucker, B. S. Mitchell and J. Spychala, *Pharmacol. Ther.*, 2005, 107, 1-30.
2. V. Bianchi, E. Pontis and P. Reichard, *Proc. Natl. Acad. Sci. U. S. A.*, 1986, 83, 986-990.
3. S. Eriksson, *Curr. Med. Chem.*, 2013, 20, 4241-4248.
4. P. Bianchi, E. Fermo, F. Alfinito, C. Vercellati, M. Baserga, F. Ferraro, I. Guzzo, B. Rotoli and A. Zanella, *Br. J. Haematol.*, 2003, 122, 847-851.
5. K. Wallden, P. Stenmark, T. Nyman, S. Flodin, S. Graslund, P. Loppnau, V. Bianchi and P. Nordlund, *J. Biol. Chem.*, 2007, 282, 17828-17836.
6. V. Bianchi and J. Spychala, *J. Biol. Chem.*, 2003, 278, 46195-46198.
7. S. A. Hunsucker, J. Spychala and B. S. Mitchell, *J. Biol. Chem.*, 2001, 276, 10498-10504.
8. C. M. Galmarini, J. R. Mackey and C. Dumontet, *Leukemia*, 2001, 15, 875-890.
9. D. A. Carson, C. J. Carrera, D. B. Wasson and T. Iizasa, *Biochim. Biophys. Acta*, 1991, 1091, 22-28.
10. S. Yamamoto, T. Yamauchi, Y. Kawai, H. Takemura, S. Kishi, A. Yoshida, Y. Urasaki, H. Iwasaki and T. Ueda, *Int. J. Hematol.*, 2007, 85, 108-115.
11. J. A. Meyer, J. Wang, L. E. Hogan, J. J. Yang, S. Dandekar, J. P. Patel, Z. Tang, P. Zumbo, S. Li, J. Zavadil, R. L. Levine, T. Cardozo, S. P. Hunger, E. A. Raetz, W. E. Evans, D. J. Morrison, C. E. Mason and W. L. Carroll, *Nat. Genet.*, 2013, 45, 290-294.
12. G. Tzoneva, A. Perez-Garcia, Z. Carpenter, H. Khiabani, V. Tosello, M. Allegretta, E. Paietta, J. Racevskis, J. M. Rowe, M. S. Tallman, M. Paganin, G. Basso, J. Hof, R. Kirschner-Schwabe, T. Palomero, R. Rabadan and A. Ferrando, *Nat. Med.*, 2013, 19, 368-371.
13. H. K. Erdemli, B. Adam and N. Bavbek, *Acta Medica (Hradec Kralove)*, 2004, 47, 129-131.
14. G. Moyle, *Clin. Ther.*, 2000, 22, 911-936; discussion 898.
15. W. Lewis and M. C. Dalakas, *Nat. Med.*, 1995, 1, 417-422.
16. W. Lewis, B. J. Day and W. C. Copeland, *Nat Rev Drug Discov*, 2003, 2, 812-822.
17. K. Brinkman, H. J. ter Hofstede, D. M. Burger, J. A. Smeitink and P. P. Koopmans, *AIDS*, 1998, 12, 1735-1744.
18. C. Mazzon, C. Rampazzo, M. C. Scaini, L. Gallinaro, A. Karlsson, C. Meier, J. Balzarini, P. Reichard and V. Bianchi, *Biochem. Pharmacol.*, 2003, 66, 471-479.
19. A. Hampton, F. Perini and P. J. Harper, *Biochemistry (Mosc)*. 1973, 12, 1730-1736.

20. E. P. Garvey, G. T. Lowen and M. R. Almond, *Biochemistry (Mosc)*, 1998, 37, 9043-9051.
21. M. Meurillon, Z. Marton, A. Hospital, L. P. Jordheim, J. Bejaud, C. Lionne, C. Dumontet, C. Perigaud, L. Chaloin and S. Peyrottes, *Eur J Med Chem*, 77, 18-37.
22. D. Rejman, A. Rabatinova, A. R. Pombinho, S. Kovackova, R. Pohl, E. Zbornikova, M. Kolar, K. Bogdanova, O. Nyc, H. Sanderova, T. Latal, P. Bartunek and L. Krasny, *J. Med. Chem.*, 2011, 54, 7884-7898.
23. D. Rejman, N. Panova, P. Klener, B. Maswabi, R. Pohl and I. Rosenberg, *J. Med. Chem.*, 2012, 55, 1612-1621.
24. Z. Tocik, I. Dvorakova, R. Liboska, M. Budesinsky, M. Masojdkova and I. Rosenberg, *Tetrahedron*, 2007, 63, 4516-4534.
25. D. Rejman, P. Kocalka, M. Budesinsky, R. Pohl and I. Rosenberg, *Tetrahedron*, 2007, 63, 1243-1253.
26. D. Rejman, P. Kocalka, M. Budesinsky, I. Barvik and I. Rosenberg, *Tetrahedron-Asymmetry*, 2007, 18, 2165-2174.
27. O. Pav, I. Barvik, M. Budesinsky, M. Masojdkova and I. Rosenberg, *Organic Letters*, 2007, 9, 5469-5472.
28. R. Liboska, M. Masojdkova and I. Rosenberg, *Collection of Czechoslovak Chemical Communications*, 1996, 61, 313-332.
29. S. Kralikova, M. Budesinsky, I. Tomeckova and I. Rosenberg, *Tetrahedron*, 2006, 62, 9742-9750.
30. A. Kralikova, M. Budesinky, M. Masojdkova and I. Rosenberg, *Tetrahedron*, 2006, 62, 4917-4932.
31. M. Endova, M. Masojdkova, M. Budesinsky and I. Rosenberg, *Tetrahedron*, 1998, 54, 11187-11208.
32. M. Endova, M. Masojdkova, M. Budesinsky and I. Rosenberg, *Tetrahedron*, 1998, 54, 11151-11186.
33. I. Kosiova, O. Simak, N. Panova, M. Budesinsky, M. Petrova, D. Rejman, R. Liboska, O. Pav and I. Rosenberg, *Eur J Med Chem*, 74, 145-168.
34. R. Liboska, M. Masojdkova and I. Rosenberg, *Collection of Czechoslovak Chemical Communications*, 1996, 61, 778-790.
35. A. Rinaldo-Matthis, C. Rampazzo, J. Balzarini, P. Reichard, V. Bianchi and P. Nordlund, *Mol. Pharmacol.*, 2004, 65, 860-867.
36. P. Pacht, M. Fabry, I. Rosenberg, O. Simak, P. Rezacova and J. Brynda, *Acta Crystallographica Section D-Biological Crystallography*, 2013, Accepted.
37. R. A. McClelland, G. Patel and P. W. K. Lam, *J. Org. Chem.*, 1981, 46, 1011-1012.
38. W. A. Sheppard, *Tetrahedron*, 1971, 27, 945-&.
39. K. H. G. Brinkhaus, E. Steckhan and D. Degner, *Tetrahedron*, 1986, 42, 553-560.
40. R. Breslow and P. S. Pandey, *J. Org. Chem.*, 1980, 45, 740-741.
41. I. Barba, R. Chinchilla and C. Gomez, *Tetrahedron*, 1990, 46, 7813-7822.
42. M. R. S.L., *MSPin*, 1.2.1-49 edn., 2008.
43. E. Diez, J. Sanfabian, J. Guilleme, C. Altona and L. A. Donders, *Molecular Physics*, 1989, 68, 49-63.
44. D. Rai, M. Johar, N. C. Srivastav, T. Manning, B. Agrawal, D. Y. Kunitomo and R. Kumar, *J. Med. Chem.*, 2007, 50, 4766-4774.
45. Y. K. Wang, D. X. Wang, C. H. Xu, R. Wang, J. J. Han and S. Y. Feng, *Journal of Organometallic Chemistry*, 2011, 696, 3000-3005.
46. M. Kalek, M. Jezowska and J. Stawinski, *Advanced Synthesis & Catalysis*, 2009, 351, 3207-3216.

47. K. L. Billingsley, T. E. Barder and S. L. Buchwald, *Angewandte Chemie-International Edition*, 2007, 46, 5359-5363.
48. R. A. Copeland, *Enzymes : a practical introduction to structure, mechanism, and data analysis*, Wiley, New York, 2nd edn., 2000.
49. A. Rinaldo-Matthis, C. Rampazzo, P. Reichard, V. Bianchi and P. Nordlund, *Nat. Struct. Biol.*, 2002, 9, 779-787.
50. K. Wallden, B. Ruzzenente, A. Rinaldo-Matthis, V. Bianchi and P. Nordlund, *Structure*, 2005, 13, 1081-1088.
51. M. R. Scholfield, C. M. Zanden, M. Carter and P. S. Ho, *Protein Sci.*, 2013, 22, 139-152.
52. P. Auffinger, F. A. Hays, E. Westhof and P. S. Ho, *Proc. Natl. Acad. Sci. U. S. A.*, 2004, 101, 16789-16794.
53. P. Politzer, P. Lane, M. C. Concha, Y. G. Ma and J. S. Murray, *J. Mol. Model.*, 2007, 13, 305-311.
54. A. Hnizda, R. Sklenickova, P. Pachl, M. Fabry, Z. Tosner, J. Brynda and V. Veverka, *Biomolecular NMR assignments*, 2013.